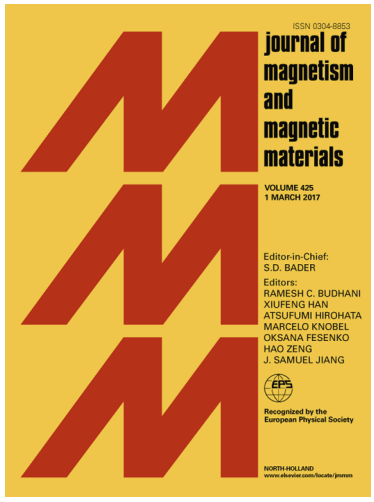

Enhanced magnetocaloric effect tuning efficiency in Ni-Mn-Sn alloy ribbons.

A. Quintana-Nedelcos, J.L. Sánchez Llamazares, G. Daniel-Perez

PII: S0304-8853(17)30638-8
DOI: http://dx.doi.org/10.1016/j.jmmm.2017.05.070
Reference: MAGMA 62774

To appear in: *Journal of Magnetism and Magnetic Materials*

Received Date: 17 February 2017
Revised Date: 2 May 2017
Accepted Date: 24 May 2017

Please cite this article as: A. Quintana-Nedelcos, J.L. Sánchez Llamazares, G. Daniel-Perez, Enhanced magnetocaloric effect tuning efficiency in Ni-Mn-Sn alloy ribbons., *Journal of Magnetism and Magnetic Materials* (2017), doi: http://dx.doi.org/10.1016/j.jmmm.2017.05.070

Enhanced magnetocaloric effect tuning efficiency in Ni-Mn-Sn alloy ribbons.

A. Quintana-Nedelcos,[1] J. L. Sánchez Llamazares,[2] G. Daniel-Perez,[3]

[1]*Department of Materials Science and Engineering, University of Sheffield, Sheffield S1 3JD, United Kingdom*
[2]*Instituto Potosino de Investigación Científica y Tecnológica A.C., Camino a la Presa San José 2055, Col. Lomas 4ª, San Luis Potosí, S.L.P. 78216, Mexico*
[3]*Instituto Tecnologico Superior de Irapuato (ITESI), 36821 Irapuato, Guanajuato, Mexico.*

Abstract. The present work was undertaken to investigate the effect of microstructure on the magnetic entropy change of $Ni_{50}Mn_{37}Sn_{13}$ ribbon alloys. Unchanged sample composition and cell parameter of austenite allowed us to study strictly the correlation between the average grain size and the total magnetic field induced entropy change (ΔS_T). We found that a size-dependent martensitic transformation tuning results in a wide temperature range tailoring (> 40 K) of the magnetic entropy change with a reasonably small variation on the peak value of the total field induced entropy change. The peak values varied from 6.0 $Jkg^{-1}K^{-1}$ to 7.7 $Jkg^{-1}K^{-1}$ for applied fields up to 2 T. Different tuning efficiencies obtained by diverse MCE tailoring approaches are compared to highlight the advantages of the herein proposed mechanism.

Keywords: Ni-Mn-Sn melt-spun ribbons; magnetocaloric effect; martensitic transformation; tuning efficiency.

I. INTRODUCTION

Ferromagnetic shape memory alloys (FSMA) have been extensively investigated in the last twenty years [1]. These materials show a structural martensitic transition (MT) from a higher temperature parent phase (austenite; AST) to the lower temperature phase (martensite; MST) accompanied by a significant abrupt magnetization jump. One of the most studied FSMA are those of the Ni–Mn–Ga system [1][2]. However, later important efforts have been carried out to find Ga-free Heusler alloys. These have been mainly focused on Ni-Mn-X system alloys, with X=Sn, In, Sb [3][4][5][6][7]. These alloys have several attractive multifunctional properties such as: inverse giant magnetocaloric-effects (MCE) [8][9][10], large magnetoresistance change [11][12], magnetic field-induced reverse martensitic transformation [13][14][15][16], magnetic superelasticity [9][17], exchange bias effect [18][19][20], and kinetic arrest of martensitic transformation [15][20][21].

Regarding potential magnetic-cooling applications, a table-like MCE for ideal Ericsson refrigeration cycles is one of the most desired features. A suitable approach to obtain a table-like MCE consists on fabricating composite materials made of constituents with tuned transition temperatures (TT) and similar total magnetic field induced magnetic entropy change (ΔS_T) [22][23][24][25]. As a case in point, in soft magnetic $Fe_{91-x}Mo_8Cu_1B_x$ (x = 15, 17, 20) amorphous alloys, the shift in Curie temperature (T_C) was reported as approximately 85 K without altering the ΔS_T peak value (ΔS_T^{max}) [23]. In Gd-Co amorphous ribbons with Gd/Co ratios from 71:29 to 62:38, T_C increases from 166K to 193K when ΔS_T^{max} slightly decreases from -3.1 $Jkg^{-1}K^{-1}$ to -2.8 $Jkg^{-1}K^{-1}$ [25]. In $Mn_{2-x}Cr_xSb$ ($0.06 \leq x \leq 0.12$), in which the MCE is given by an antiferro to ferri-magnetic first-order phase transition (FOPT), with the increases on Cr content the transition temperature shifts from 232K to 333K and ΔS_T^{max} decreases from 7.5 $Jkg^{-1}K^{-1}$ to 5.5 $Jkg^{-1}K^{-1}$[24].

Even though in Ni-Mn-X (X=Sn, In, Sb) FSMA significant efforts have been effectively implemented to tune the MT through the change of the Mn/X ratio [4][5][6], the partial atomic substitution of one (or more) of the three main elements of the alloy [26][27][28][29][30] and the introduction of elements of small atomic radius into interstitial sites [31][32]). However, these methods have failed in keeping reasonable unchanged the ΔS_T^{max}. Table 1 shows the peak value of the total field induced magnetic entropy change (ΔS_T^{max}) together with the corresponding

order-disorder MT temperature reported for different Ni-Mn-Sn bulk samples. The considerable effect of the different MT tuning mechanisms on the ΔS_T^{max} is clearly observed.

Table 1. Reported transition temperature and ΔS_T^{max} values related to their transition path for some Ni-Mn-Sn bulk alloys.

Alloy composition	Transition path	Trans. temp. (K)	ΔS_T^{max} ($Jkg^{-1}K^{-1}$)	Ref.
$Ni_{43}Mn_{45}Sn_{11}B_x$			$\mu_o \Delta H_{max}$ = 1 T	[31]
x=0	MST → AST	200*	10.4	
x=1	MST → AST	215*	13.0	
x=3	MST → AST	242*	6.5	
x=5	MST → AST	275*	2.2	
$Ni_{43}Mn_{46-x}Cu_xSn_{11}$			$\mu_o \Delta H_{max}$ = 1 T	[26]
x=1	MST → AST	226**	14.1	
x=2	MST → AST	255**	18.0	
x=3	MST → AST	260**	15.8	
$Ni_{50}Mn_{50-x}Sn_x$				
x=13	AST → MST	307*	18; $\mu_o \Delta H_{max}$ = 5 T	[8]
x=15	AST → MST	192*	15; $\mu_o \Delta H_{max}$ = 5 T	[8]
x=16	MST → AST	220***	2.0; $\mu_o \Delta H_{max}$ = 8 T	[33]
$Ni_{50-x}Mn_{39+x}Sn_{11}$			$\mu_o \Delta H_{max}$ = 1 T	[34]
x=5	AST → MST	270*	6.8	
x=6	AST → MST	245*	10.1	
x=7	AST → MST	200*	10.1	

*M_s, **A_f, ***temperature of ΔS_T^{max}

Evidence indicates that the tuning mechanisms do not only strongly influence the MT shift, they also affect considerable the ΔS_T^{max} magnitudes. The latter could be due to uncontrolled variables that may directly influence the thermo-magnetic response of the material. For instance, the high dispersion obtained in average grain sizes $\langle d \rangle$ in Ni-Mn-Sn bulk samples (50 μm ≤ $\langle d \rangle$ ≤ 300 μm) does not allow to study the effect of this parameter on the thermo-magnetic features of these materials [3][35][36].

On the other hand, it has been established that the melt spinning technique is an effective process to obtain single phase alloy ribbons in the $Ni_{50}Mn_{50-x}Sn_x$ system [16][37][38] with a considerably refined microstructure [4][36]. The technique reasonably reproduces the MCE properties of the bulk alloys while reducing the characteristic martensitic starting (M_s) and austenitic starting (A_s) transformation temperatures. For example, for $Ni_{50}Mn_{37}Sn_{13}$ bulk samples, ΔS_T^{max} has been reported as ~ 8 $Jkg^{-1}K^{-1}$ (at $\mu_o \Delta H_{max}$ = 2 T) [8] with M_s near room temperature (RT), 290 K [36] and 307 K [8][35]; while ΔS_T^{max} = 10 $Jkg^{-1}K^{-1}$ ($\mu_o \Delta H_{max}$ = 2 T) [39] and M_s =

218 K [37] for alloy ribbons of similar composition. Further studies in Ni-Mn-Sn ribbons [40][41] and thin films [42][43] have confirmed the magneto-structural transition dependence on <*d*>.

The present work has been carried out to continue and expand previous results reported in [41], in wich the authors demonstrated that for $Ni_{50}Mn_{37}Sn_{13}$ ribbons with decreased <*d*>, the multivariant MT temperature shifts downward due to the stabilization of the AST phase. The experiment was carefully designed to study the viability of tunning the MT in $Ni_{50}Mn_{37}Sn_{13}$ ribbons by controlling solely its microstructural features (i..e. average grain size) while keep unaffected structural and compositional parameters. In turns, undesired variables contribution to the MT tunning is minimized. For instances, existing phase (single highly-ordered $L2_1$-type AST cubic structure), stress relaxation (fair constant lattice parametter a = 5.970 +/- 0.005 Å) and chemical deviation (average valence electron concentration per atom e/a = 8.12 +/- 0.01) parametters show to have a negligible impact on the MT shift in our experiment. As such, it was proven that the decrease in M_S from 258 K to 212 K (i.e., 46 K) can be strictly ascribed to the austenite stabilization due to the reduction in the grain size [41]. As present contribution is built on [41] outcomes, herein propossal aims to evaluate the ΔS_T^{max} tuning efficiency by means of the MT dependece on <*d*>.

II. EXPERIMENTAL PROCEDURE

Alloy ribbons with 1.4 μm ≤ <*d*> ≤ 7.3 μm obtained by varying wheel speed (ranging from 50 ms^{-1} to 15 ms^{-1}) where prepared from bulk ingots of $Ni_{50}Mn_{37}Sn_{13}$ nominal composition. They were annealed in closed quartz ampoules at 1123 K (850 ^oC) for 10 min under high vacuum to improve atomic ordering. Microstructural characterization was done in a Phillips model XL-30 scanning electron microscope (SEM). Structural analysis by phase transition studies were carried out by differential scanning calorimeter (DSC) using a TA Instruments model Q200. Additional information on ribbons fabrication and characterization can be found elsewhere [41].

Magnetization measurements were performed using the vibrating sample magnetometer option of a physical properties measurement system (Quantum Design PPMS® EverCool-I, 9 Tesla). The magnetic field *H* was applied along the ribbon axis (i.e., the rolling direction) to minimize demagnetizing field effects. The magnetization as a function of temperature $\sigma(T)$ curves were

determined following field-cooling (FC), and field-heating (FH) regimens under an applied magnetic field of 5 mT. The heating/cooling rate was 1.0 $Kmin^{-1}$. Magnetization isotherms were measured through the MST-to-AST phase transition up to 5 T. The total field-induced magnetic entropy change $\Delta S_T(T)$ curves were obtained from a set of $M(\mu_o H)$ isotherms by applying the Maxwell relation (equation 1). A fixed thermal protocol, referred in [44] as BnF, was used to reach each measuring temperature T_{measur}.

$$\left(\frac{\partial S}{\partial B}\right)_T = \left(\frac{\partial M}{\partial T}\right)_B \rightarrow \Delta S_T = \int_0^B \left(\frac{\partial M}{\partial T}\right)_B dB \qquad \text{(equation 1)}$$

III. EXPERIMENTAL RESULTS AND DISCUSSION

Figures 1a and 1b show SEM images of the free-surface microstructure of the ribbons obtained at copper linear speeds of 15 and 50 ms^{-1}, respectively. More than 200 measurements of the free surface were used to estimate the average grain diameter, $<d>$ = 7.3 +/- 3.4 μm and 1.4 +/- 0.6 μm for the Sn15TT and Sn50TT ribbons, respectively. The inset images show histograms of the measured grain diameters as determined from SEM images.

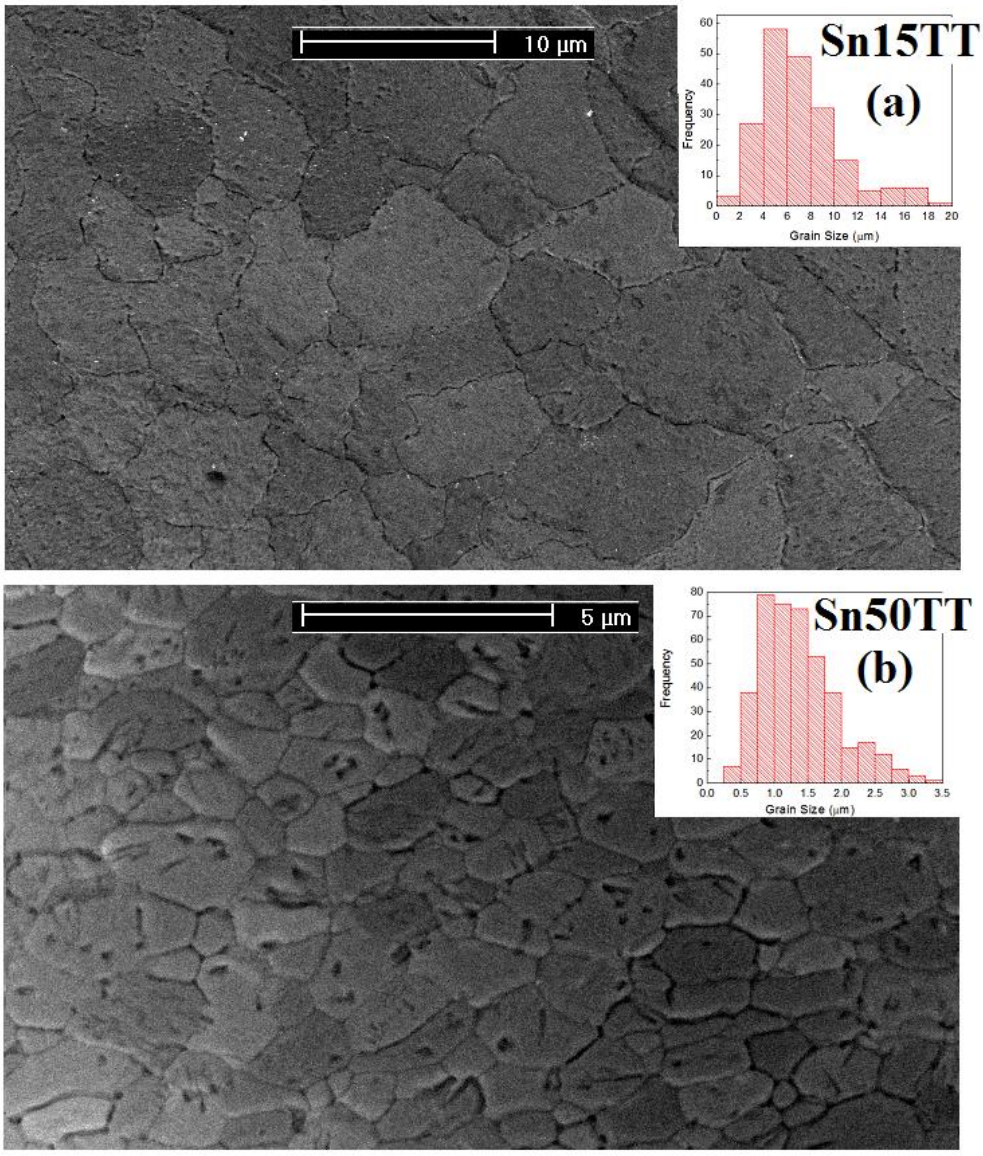

Fig 1. Typical SEM images showing the surface microstructure of ribbons on their free surface (i.e., non-contact side, NCS). Insets: Histogram of grain sizes measured from SEM micrographs.

Figures 2a and 2b show the DSC and low-field magnetization curves of the Sn15TT and Sn50TT samples, respectively. The thermal hysteresis of the magnetization curves indicates the first-order behaviour of the transition. On both sets of curves, the two well-distinct MST and AST ferromagnetic regions and the jump in magnetization associated to the structural phase transition are observed. The AST Curie temperature T^{A}_{C} is found to be 313 K for both samples. As revealed, the coupled magneto-structural transition shifts to lower temperatures with the decrease of $<d>$. The latter was explained under a phenomenological model consideration in which the decrease in the average grain size stabilizes the austenitic parent phase [41]. The

experiment was carefully designed to minimize the undesired contribution of changes in the elemental chemical composition and cell parameter of AST on the magneto-structural transition features. Experimental details on the procedure can be found elsewhere [41].

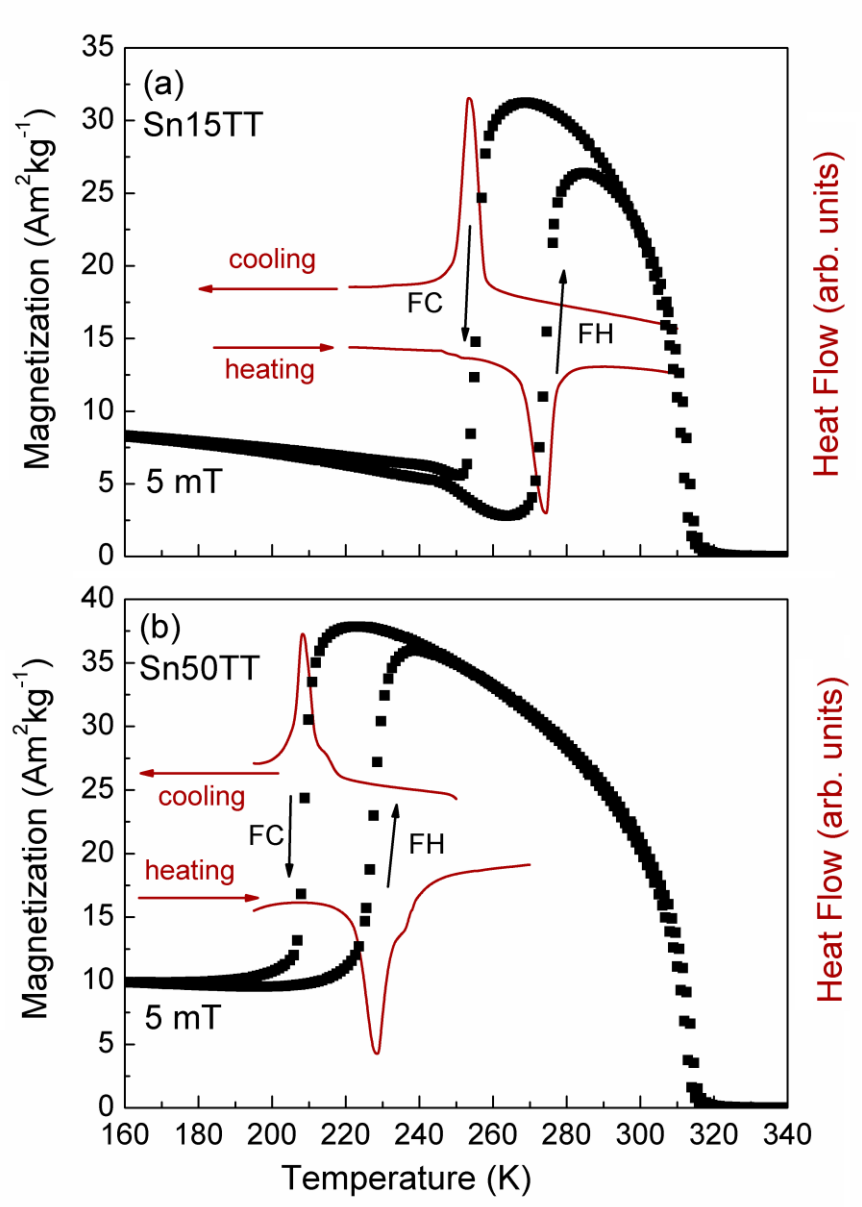

Fig 2. FC and FH temperature dependence of the magnetization M(T) at 5 mT and DSC curves of (a) Sn15TT and (b) Sn50TT ribbons.

Figures 3a and 3b show the magnetizing (FU) $M(\mu_o H)$ curves for the Sn15TT and Sn50TT alloy ribbons, respectively. In both samples, $M(\mu_o H)$ curves were computed across the reverse martensitic transformation (i.e. MST → AST) with a temperature step of 1.5 K between consecutive measuring temperatures (T_{measur}) and an increasing applied field from 0 to $\mu_o H_{max}$ = 5T. To ensure that the sample reaches every T_{measur} following the same thermal and magnetic

history, at zero magnetic field the sample was first warmed up to a completely AST-paramagnetic state at T = 400 K, followed by a cooling to a MST-ferromagnetic phase at T =180K, before heated up to the next T_{measur}. This thermal cycle is repeated after every $M(\mu_o H)$ measurement. $\Delta S_T(T)$ curves obtained from these $M(\mu_o H)$ measurements are shown in Fig. 4.

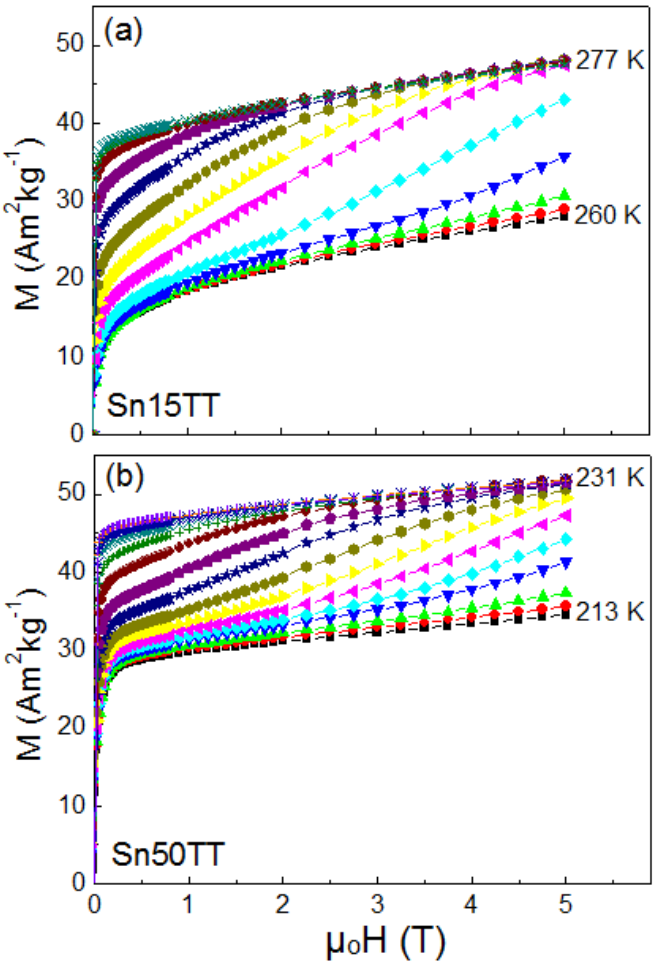

Fig 3. Isothermal magnetization $M(\mu_o H)$ curves of (a) Sn15TT and (b) Sn50TT alloy ribbons for increasing field across the reverse martensitic transformation.

For sample Sn15TT (Sn50TT), ΔS_T^{max} is found to be equal to 7.7 Jkg^{-1}K^{-1} (6.0 Jkg^{-1}K^{-1}) and 14.0 Jkg^{-1}K^{-1} (11.2 Jkg^{-1}K^{-1}) for $\mu_o \Delta H_{max}$ = 2 T and 5 T, respectively. These magnitudes are comparable to others previously reported for alloys of similar composition. For instance, ΔS_T^{max} = 6.1 Jkg^{-1}K^{-1} [45] and 10 Jkg^{-1}K^{-1} [39] for alloy ribbons of $Ni_{49.0}Mn_{37.4}Sn_{13.6}$ and $Ni_{50}Mn_{37}Sn_{13}$, respectively and ΔS_T^{max} = 8 Jkg^{-1}K^{-1} for $Ni_{50}Mn_{37}Sn_{13}$ bulk alloys [8]. All of them calculated for an applied field change of 2 T. Moreover, a more important result than the calculated ΔS_T^{max} magnitude of our samples is the relatively small variation of this physical quantity across the

temperature window herein studied. In our samples, a shift of ΔA_s = 42 K is obtained at a cost of 1.7 Jkg^{-1}K^{-1} (for $\mu_o \Delta H_{max}$ = 2 T) and 3.0 Jkg^{-1}K^{-1} (for $\mu_o \Delta H_{max}$ = 5 T) on ΔS_T^{max}. The increase of ΔS_T^{max} in samples with higher MT can be ascribed to the shorter temperature proximity of A_s to T^A_C [46]. It's worth noting that the irreversibly dissipated energy slightly rise from 7.1 % to 9.4 % while the thermal hysteresis of the transformation remains similar (within the measurement error) with the decrease of <*d*> from 7.3 μm (Sn15TT) to 1.4 μm (Sn50TT). For further details of the effect of microstructure on transformation parameters see reference [41].

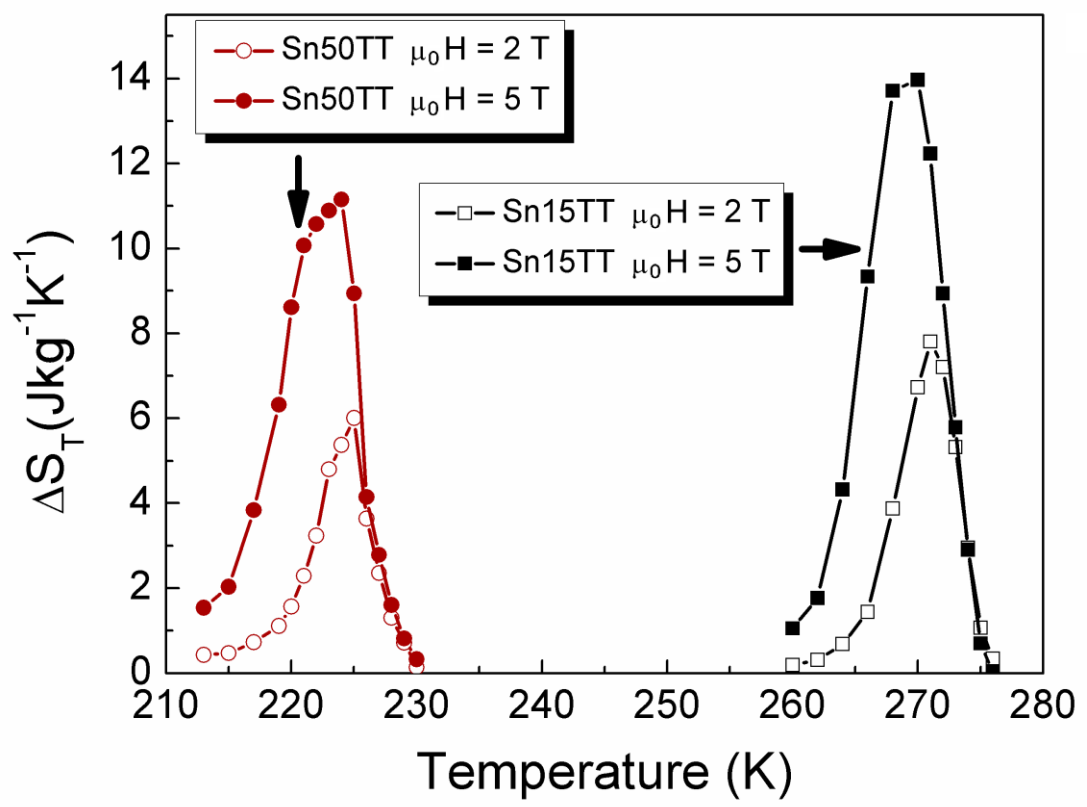

Fig 4. Total field-induced magnetic entropy change as a function of temperature $\Delta S_T(T)$ under an applied magnetic field change of 2 T and 5 T.

For comparative assessment, we can define the tuning efficiency (T_e = $\left|\Delta TT/\Delta(\Delta S_T^{max})\right|$) as the TT shifted interval at the expense of a ΔS_T^{max} variation of 1 Jkg^{-1}K^{-1}. For practical purposes, TT can be any of the characteristic transition temperatures of the magneto-structural transition (i.e., martensitic starting M_S, martinsitic finishing M_f, austenitic starting A_S, austenitic finishing A_f, among others). For example, for interstitially doped $Ni_{43}Mn_{45}Sn_{11}B_x$ bulk samples, M_S shifts from 200 K (x = 0) to 245 K (x = 3); while ΔS_T^{max} decreases from 10.4 Jkg^{-1}K^{-1} to 6.5 Jkg^{-1}K^{-1}

[31] at T_e = 11.5 $J^{-1}kgK^2$. A comparison of estimated TT, ΔS_T^{max}, and T_e for both ribbons studied in the present work (PW) and other research groups are listed in Table 2.

Table 2. Reported transition temperature (TT), ΔS_T^{max} and, T_e values related to their transition path for some Ni-Mn-Sn system alloy ribbons. Dashed squeares enclose the data used for the T_e calculation.

Alloy composition	Transition path	TT (K)	ΔS_T^{max} ($Jkg^{-1}K^{-1}$)	T_e ($J^{-1}kgK^2$)	Ref.
			$\mu_o\Delta H_{max}$ = 5 T		PW
Sn15TT	MST → AST	267***	14	24.7	
Sn50TT	MST → AST	225***	11		
			$\mu_o\Delta H_{max}$ = 2 T		PW
Sn15TT	MST → AST	267***	7.7	14.0	
Sn50TT	MST → AST	225***	6.0		
$Ni_{49.0}Mn_{37.4}Sn_{13.6}$	MST → AST	297.5**	$\mu_o\Delta H_{max}$ = 2 T 6.1		[45]
$Ni_{50.3}Mn_{35.5}Sn_{14.4}$	MST → AST	237***	$\mu_o\Delta H_{max}$ = 2 T 4.1		[47]
$Ni_{48}Mn_{39.5}Sn_{12.5-x}Al_x$			$\mu_o\Delta H_{max}$ = 2 T		[18]
x=0	MST → AST	269**	7.8		
x=1	MST → AST	287**	5.7		
x=2	MST → AST	306**	4.8	9.0	
x=3	MST → AST	314**	2.8		
$Ni_{44.1}Mn_{44.2}Sn_{11.7}$			$\mu_o\Delta H_{max}$ = 1 T		[38]
As-quenched	MST → AST	230****	~ 7		
TA[a] – A	MST → AST	235****	~ 32	2.5	
TA[a] – B	MST → AST	265****	~ 20		
$Ni_{50-x}Fe_xMn_{40}Sn_{10}$			$\mu_o\Delta H_{max}$ = 5 T		[48]
x=2	MST → AST	377***	~ 2		
x=4	MST → AST	356***	~ 4		
x=6	MST → AST	309***	~ 7	10	
x=8	MST → AST	286***	~ 11		
$Ni_{43}Co_7Mn_{39}Sn_{11}$ WS[b] =			$\mu_o\Delta H_{max}$ = 1 T		[40]
10 ms^{-1}	MST → AST	278.05***	16.42		
WS[b] = 15 ms^{-1}	MST → AST	296.85***	17.49		
WS[b] = 20 ms^{-1}	MST → AST	296.85***	14.21	33.4	
WS[b] = 25 ms^{-1}	MST → AST	302.75***	15.68		
WS[b] = 30 ms^{-1}	MST → AST	266.05***	23.89		

*minimum of the derivative of the M(T)-FH curve; ** A_f; *** A_s; **** temperature at which ΔS_T^{max} is found; [a]Thermal Annealing; [b]Wheel Speed.

The calculated tuning efficiency of 14.0 $J^{-1}kgK^2$ (at $\mu_o\Delta H_{max}$ = 2 T) and 24.7 $J^{-1}kgK^2$ (at $\mu_o\Delta H_{max}$ = 5 T) in our samples is higher than those computed for other series where different tuning mechanism were used: Sn/Al [18] (T_e = 9.0 $J^{-1}kgK^2$; $\mu_o\Delta H_{max}$ = 2 T) and Ni/Fe [48] (T_e = 10 $J^{-1}kgK^2$; $\mu_o\Delta H_{max}$ = 5 T) partial substitution; applied diferent thermal treatments on $Ni_{44.1}Mn_{44.2}Sn_{11.7}$ alloy ribbons (T_e = 2.5 $J^{-1}kgK^2$; $\mu_o\Delta H_{max}$ = 1 T) [38]; and $Ni_{43}Mn_{45}Sn_{11}B_x$ (T_e

= 11.5 $J^{-1}kgK^2$; $\mu_o \Delta H_{max}$ = 1 T) interstitial doping [31]. Notice that T_e = 33.4 $J^{-1}kgK^2$ ($\mu_o \Delta H_{max}$ = 1 T) for ribbon samples of $Ni_{43}Co_7Mn_{39}Sn_{11}$ is considerably higher than our results. Similarly to our work, the MT was tuned through a variation of the wheel speed (WS) during the spinning process [40]. However, Ma et al, [40] obtained a non-monotonous dependence of TT on WS, which causes up-and-down unrelated values of ΔS_T^{max} with TT (see arrows in table 2). Therefore, if for the T_e computing from A_s = 278 K (WS = 10 ms^{-1}) to A_s = 303 K (WS = 25 ms^{-1}) we use the maximum (17.5 $Jkg^{-1}K^{-1}$) and minimum (14. 2 $Jkg^{-1}K^{-1}$) values reported within the temperature ΔA_S interval of 24.7 K [40], the tunning efficiency results to be 7.5 $J^{-1}kgK^2$. This is an order of magnitude smaller than that calculated from the ΔS_T^{max} values corresponding to the lower and higher A_s temperatures of the same interval (i.e., T_e = 33.4 $J^{-1}kgK^2$). However, the up-and-down values of ΔS_T^{max} should not necessary impact the tuning efficiency, provided that the peak values remain relatively close to each other.

IV. CONCLUSIONS.

In conclusion, in studying ribbons of $Ni_{50}Mn_{37}Sn_{13}$ nominal composition and different grain sizes we found that with the decrease of $<d>$ from 7.3 μm to 1.4 μm, the MCE of the material was successfully tailored in a broad range of temperatures (ΔA_S = 42 K and ΔM_S = 46 K) at a relatively small cost in terms of ΔS_T^{max} peak value. Results confirm that the MT dependence on extrinsic properties of the material (for instance, average grain size) allows a better MCE tunning efficiency than other tailoring aproaches that uses the MT dependence on instrinsic properties based on the chemical composition or structural features of the material. The latter has a significant added value as keeping nearly constant the MCE magnitude of the material is a key pre-condition in view of the potential application of these materials in magnetic refrigeration.

ACKNOWLEDGEMENTS

The authors gratefully acknowledge the financial support provided by: (a) CONACYT, Mexico, under grant CB-2012-01-183770 and CB-2012-01-0176705; (b) LINAN (IPICYT); and (c) CONACyT, Red de Nanociencias y Nanotecnología. Technical support received from M.Sc. G.J. Labrada-Delgado and B.A. Rivera-Escoto is recognized. This project was supported by the Royal

Academy of engineering under the Newton Research Collaboration Programme Reference NRCP1617/5/59.

REFERENCES

[1] J. Pons, E. Cesari, C. Seguí, F. Masdeu, and R. Santamarta, *Mater. Sci. Eng. A*, vol. 481–482, pp. 57–65, May 2008.
[2] O. Söderberg, I. Aaltio, Y. Ge, O. Heczko, and S.-. Hannula, *Mater. Sci. Eng. A*, vol. 481–482, pp. 80–85, May 2008.
[3] Y. Sutou, Y. Imano, N. Koeda, T. Omori, R. Kainuma, K. Ishida, and K. Oikawa, *Appl. Phys. Lett.*, vol. 85, no. 19, p. 4358, 2004.
[4] T. Krenke, M. Acet, E. Wassermann, X. Moya, L. Mañosa, and A. Planes, *Phys. Rev. B*, vol. 72, no. 1, p. 14412, Jul. 2005.
[5] T. Krenke, M. Acet, E. Wassermann, X. Moya, L. Mañosa, and A. Planes, *Phys. Rev. B*, vol. 73, no. 17, p. 174413, May 2006.
[6] J. Du, Q. Zheng, W. J. Ren, W. J. Feng, X. G. Liu, and Z. D. Zhang, *J. Phys. D. Appl. Phys.*, vol. 40, no. 18, pp. 5523–5526, Sep. 2007.
[7] A. K. Nayak, K. G. Suresh, and a K. Nigam, *J. Phys. D. Appl. Phys.*, vol. 42, no. 3, p. 35009, Feb. 2009.
[8] T. Krenke, E. Duman, M. Acet, E. F. Wassermann, X. Moya, L. Mañosa, and A. Planes, *Nat. Mater.*, vol. 4, no. 6, pp. 450–454, Jun. 2005.
[9] T. Krenke, E. Duman, M. Acet, E. F. Wassermann, X. Moya, L. Mañosa, A. Planes, E. Suard, and B. Ouladdiaf, *Phys. Rev. B*, vol. 75, no. 10, p. 104414, 2007.
[10] A. M. Aliev, A. B. Batdalov, I. K. Kamilov, V. V. Koledov, V. G. Shavrov, V. D. Buchelnikov, J. García, V. M. Prida, and B. Hernando, *Appl. Phys. Lett.*, vol. 97, p. 212505, 2010.
[11] V. K. Sharma, M. K. Chattopadhyay, K. H. Shaeb, A. Chouhan, and S. B. Roy, *Appl. Phys. Lett.*, vol. 89, p. 222509, 2006.
[12] K. Koyama, H. Okada, and K. Watanabe, *Appl. Phys. Lett.*, vol. 89, p. 182510, 2006.
[13] R. Kainuma, Y. Imano, W. Ito, Y. Sutou, H. Morito, S. Okamoto, O. Kitakami, K. Oikawa, a Fujita, T. Kanomata, and K. Ishida, *Nature*, vol. 439, no. 7079, pp. 957–60, Feb. 2006.
[14] K. Koyama, K. Watanabe, T. Kanomata, R. Kainuma, K. Oikawa, and K. Ishida, *Appl. Phys. Lett.*, vol. 88, no. 13, p. 132505, 2006.
[15] F. Chen, Y. X. Tong, Y. J. Huang, B. Tian, L. Li, and Y. F. Zheng, *Intermetallics*, vol. 36, pp. 81–85, May 2013.
[16] J. L. Sanchez Llamazares, A. Quintana-Nedelcos, D. Ríos-jara, and C. F. Sánchez-Valdes, *J. Magn. Magn. Mater.*, vol. 401, pp. 38–43, 2016.
[17] L. Mañosa, E. Stern-Taulats, A. Planes, P. Lloveras, M. Barrio, J.-L. Tamarit, B. Emre, S. Yüce, S. Fabbrici, and F. Albertini, *Phys. Status Solidi*, vol. 251, no. 10, pp. 2114–2119, 2014.
[18] P. Czaja, W. Maziarz, J. Przewoźnik, C. Kapusta, L. Hawelek, A. Chrobak, P. Drzymała, M. Fitta, and A. Kolano-Burian, *J. Magn. Magn. Mater.*, vol. 358–359, pp. 142–148, May 2014.
[19] R. Vishnoi and D. Kaur, *J. Alloys Compd.*, vol. 509, no. 6, pp. 2833–2837, Feb. 2011.
[20] J. L. S. Llamazares, B. Hernando, J. J. Suñol, C. García, and C. a. Ross, *J. Appl. Phys.*, vol. 107, no. 9, p. 09A956, 2010.

[21] V. Sánchez-Alarcos, V. Recarte, J. I. Pérez-Landazábal, C. Gómez-Polo, and J. a. Rodríguez-Velamazán, *Acta Mater.*, vol. 60, no. 2, pp. 459–468, Jan. 2012.
[22] P. Alavarez-Alonzo, P. Gorria, J. L. Sanchez-Llamazares, and J. A. Blanco, *J. Alloys Compd.*, vol. 568, pp. 98–101, 2013.
[23] V. Franco, C. F. Conde, J. S. Blázquez, and A. Conde, *J. Appl. Phys.*, vol. 101, no. May, p. 93903, 2007.
[24] L. Caron, X. F. Miao, J. C. P. Klaasse, S. Gama, and E. Brück, *Appl. Phys. Lett.*, vol. 103, no. 11, p. 112404, 2013.
[25] C. L. Zhang, D. H. Wang, Z. D. Han, H. C. Xuan, B. X. Gu, and Y. W. Du, *J. Appl. Phys.*, vol. 105, p. 13912, 2009.
[26] D. H. Wang, C. L. Zhang, H. C. Xuan, Z. D. Han, J. R. Zhang, S. L. Tang, B. X. Gu, and Y. W. Du, *J. Appl. Phys.*, vol. 102, no. 1, p. 13909, 2007.
[27] A. K. Nayak, K. G. Suresh, and a. K. Nigam, *J. Appl. Phys.*, vol. 107, no. 9, p. 09A927, 2010.
[28] D. H. Wang, C. L. Zhang, Z. D. Han, H. C. Xuan, B. X. Gu, and Y. W. Du, *J. Appl. Phys.*, vol. 103, no. 3, p. 33901, 2008.
[29] Z. Liu, Z. Wu, H. Yang, Y. Liu, W. Wang, X. Ma, and G. Wu, *Intermetallics*, vol. 19, no. 10, pp. 1605–1611, Oct. 2011.
[30] I. Dubenko, T. Samanta, A. Kumar Pathak, A. Kazakov, V. Prudnikov, S. Stadler, A. Granovsky, A. Zhukov, and N. Ali, *J. Magn. Magn. Mater.*, vol. 324, no. 21, pp. 3530–3534, Oct. 2012.
[31] H. C. Xuan, D. H. Wang, C. L. Zhang, Z. D. Han, B. X. Gu, and Y. W. Du, *Appl. Phys. Lett.*, vol. 92, no. 10, p. 102503, 2008.
[32] F. X. Hu, J. Wang, L. Chen, J. L. Zhao, J. R. Sun, and B. G. Shen, *Appl. Phys. Lett.*, vol. 95, no. 11, p. 112503, 2009.
[33] V. K. Sharma, M. K. Chattopadhyay, R. Kumar, T. Ganguli, P. Tiwari, and S. B. Roy, *J. Phys. Condens. Matter*, vol. 19, no. 49, p. 496207, Dec. 2007.
[34] Z. D. Han, D. H. Wang, C. L. Zhang, H. C. Xuan, B. X. Gu, and Y. W. Du, *Appl. Phys. Lett.*, vol. 90, no. 4, p. 42507, 2007.
[35] T. Krenke, M. Acet, E. Wassermann, X. Moya, L. Mañosa, and A. Planes, *Phys. Rev. B*, vol. 72, no. 1, p. 014412 1-9, Jul. 2005.
[36] D. L. Schlagel, W. M. Yuhasz, K. W. Dennis, R. W. McCallum, and T. A. Lograsso, *Scr. Mater.*, vol. 59, no. 10, pp. 1083–1086, Nov. 2008.
[37] J. D. Santos, T. Sanchez, P. Alvarez, M. L. Sanchez, J. L. Sánchez Llamazares, B. Hernando, L. Escoda, J. J. Suñol, and R. Varga, *J. Appl. Phys.*, vol. 103, no. 7, p. 07B326, 2008.
[38] H. C. Xuan, K. X. Xie, D. H. Wang, Z. D. Han, C. L. Zhang, B. X. Gu, and Y. W. Du, *Appl. Phys. Lett.*, vol. 92, no. 24, p. 242506, 2008.
[39] D. Wu, S. Xue, J. Frenzel, G. Eggeler, Q. Zhai, and H. Zheng, *Mater. Sci. Eng. A*, vol. 534, pp. 568–572, Feb. 2012.
[40] S. C. Ma, C. W. Shih, J. Liu, J. H. Yuan, S. Y. Lee, Y. I. Lee, H. W. Chang, and W. C. Chang, *Acta Mater.*, vol. 90, no. 10 pp. 292–302, 2015.
[41] A. Quintana-Nedelcos, J. L. Sánchez-lamazares, D. Ríos-Jara, A. G. Lara-Rodríguez, and T. García-Fernández, *Phys. Status Solidi*, vol. 210, pp. 2159–2165, 2013.
[42] R. Vishnoi, R. Singhal, and D. Kaur, *J. Nanoparticle Res.*, vol. 13, no. 9, pp. 3975–3990, Mar. 2011.
[43] A. Quintana-Nedelcos, J. L. Sanchez-Llamazares, T. García-Fernández, S. Guvenc, M. Yumak, and C. García, *J. Sci. Res. Reports*, vol. 6, no. 6, pp. 476–482, 2015.

[44] A. Quintana-Nedelcos, J. L. Sánchez Llamazares, C. F. Sánchez-Valdés, P. Álvarez Alonso, P. Gorria, P. Shamba, and N. A. Morley, *J. Alloys Compd.*, vol. 694, pp. 1189–1195, 2017.
[45] I. Babita, R. Gopalan, S. Ram, and H.-J. Fecht, *Nanosci. Nanotechnol. Lett.*, vol. 1, no. 3, pp. 151–155, Dec. 2009.
[46] P. Czaja, M. Fitta, J. Przewoznik, W. Maziarz, J. Morgiel, T. Czeppe, and E. Cesari, *Acta Mater.*, vol. 103, pp. 30–45, 2016.
[47] B. Hernando, J. L. Sánchez Llamazares, J. D. Santos, V. M. Prida, D. Baldomir, D. Serantes, R. Varga, and J. González, *Appl. Phys. Lett.*, vol. 92, no. 13, p. 132507, 2008.
[48] C. O. Aguilar-Ortiz, D. Soto-Parra, P. Alvarez-Alonzo, P. Lazpita, D. Salazar, P. O. Castillo-Villa, H. Flores-Zuñiga, and V. . A. Chernenko, *Acta Mater.*, vol. 107, pp. 9–16, 2016.

Highlights

- We compare the MCE tuning efficiency of different tailoring approaches.
- Changing extrinsic properties allows a better MCE tunning efficiency.